MEDWIN PUBLISHERS
Committed to create value for Researchers

International Journal of Zoology and Animal Biology
ISSN: 2639-216X

A Computational Model for the Study of Release Call in the Pyrenean High Mountain European Common Frog (*Rana Temporaria*)

Palanca-Castan N[1], Miramontes-Sequeiros LC[2]* and Palanca-Soler A[2]

[1]University of Valparaiso, Chile

[2]Department of Ecology and Animal Biology, University of Vigo, Spain

***Corresponding author:** Luz Calia Miramontes Sequeiros, Department of Ecology and Animal Biology, Faculty of Biology, University of Vigo, Animal Anatomy Laboratory Foundation, Spain; Email: luz.miramontes@outlook.es

Research Article

Volume 2 Issue 4

Received Date: July 27, 2019

Published Date: August 09, 2019

DOI: 10.23880/izab-16000169

Abstract

The aim of this study was to develop a computational model to perform a bioacoustic characterization of the release call of a high-mountain population of *Rana temporaria*. We also wanted to determine the way in which variation in specific anatomical structures, such as the nostrils and mouth cavities, affected call structure. For this purpose, we recorded induced release calls, above- and underwater, of individual frogs all over our research area as well as additional biometric data in the form of photographs, radiographs and video recordings. The data collected were used to create a virtual synthesized call that could replicate them, taking into account the variation introduced by the natural anatomical structures. Our model successfully replicated the recorded calls. We determined the role of mouth cavity acting as a Helmholtz resonator, both above and underwater, which suppressed certain frequency groups in order to highlight those with biological relevance. We also determined the role of the nasal cavities, which acted as a tube resonator amplifying specific frequencies during above-water vocalizations. The nasal cavity remained closed and therefore did not act as a resonator during underwater vocalizations.

Keywords: European Common Frog; Release Call; Virtual Simulation; Computational Model; Pyrenees

Introduction

Recent works have dealt with the study of the release call in different anuran such as *Rhinella margaritifera*, *Pelobates varaldii* or *P. fuscus*, *P. syriacus* and *P. cultripes*, but little is known about *Rana temporaria* [1-3]. Calling frogs face the challenge of transmitting a clear signal signal clearly in an environment filled with natural noises as well as calls from other frogs from the same and different species. Frogs use two main strategies used to overcome this challenge: a: increase the signal-to-noise ratio and/or the intensity of the call by changing the structural properties of the signal and b: increase the redundancy of the communication by elongating or repeating a given call [4]. The present paper deals with the first strategy by studying the structural properties of individual calls from a high-mountain population of *Rana*

temporaria located in the Spanish Pyrenees. Individuals of *R. temporaria* usually only emit spontaneous vocalizations when underwater, which led us to use induced, above-water release calls for the purposes of this study. The males of several frog species also emit underwater vocalizations, which are adapted to the transmission properties of the medium so they can propagate in shallow waters [5]. We expected our study population to present similar characteristics. Frogs typically produce calls via muscular contractions of the body wall, which force air from the lungs and through the larynx towards the vocal sacs. However, sound production is not limited to the vocal sacs. In many species, such as *R. temporaria*, the tympanic membranes also have a role in sound production [6]. In addition, the following anatomical structures can also have an important role in defining the structural properties of vocalizations:

A. Mouth Cavity: the mouth cavity in Anurans is formed by several bones that define the skull and suspensorium [7,8] and form a cavity in roughly the shape of a rectangular prism (Figure 1). In the dorsal surface we can find the parietal nasal bones, which border in their posterior part with the sphenethmoid, which itself is anterior to the front parietals, which make contact with the anterior part of the exoccipitals and prootics. In the ventral surface, opposite to the sphenetmoid, we can find the premaxillaries, maxillaries, vomer and palatine, located anterior to the parasphenoid. The lower jaw is formed by the mentomeckelian bone in the apex, as well as by the dentaries. The maxillary bones project posteriorly, ending in contact with the quadratojugal. The quadratojugal is in contact with the pterygoid, and both of them form the suspensorium. The pterygoid has three branches in the form of a Y, which make contact with the prootic, the exoccipital, the squamous, the quadratojugal and the angulosplenial. In amphibians, two main types of mouth movements can be distinguished: strong contractions that inflate the lungs, and shallow oscillatory movements that ventilate the nasal cavity, bringing parts of the medium (whether air or water) to the chemoreceptors. Of these, the strong contraction is less frequent.

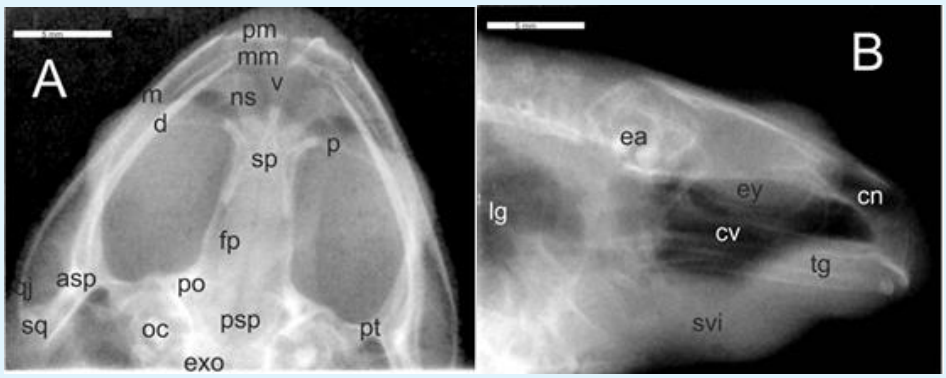

Figure 1: A: Dorsoventral radiograph of the head of *R. temporaria*. **ns**: nasal; **sp**: sphenethmoid; **fp**: frontoparietals; **exo:** exoccipital; **po:** prootic; **pm:** premaxilla; **m:** maxillar; **v:** vomer; **p:** palatine; **psp:** parasphenoid; **mm:** mentomeckelian; **d:** dentary; **qj:** quadratojugal; **pt:** pterygoid; **sq:** squamosal; **asp:** angulosplenial; **oc:** otic capsules; **B:** Lateral radiograph of the head of *R. temporaria*; **cv:** mouth cavity; **cn:** nasal cavity; **tg:** tonge; **lg:** lungs; **ea:** ears; **ey:** eyes; **svi:** internal vocal sacs.

B. Nasal Cavities: the paired nose cavities in Anurans are formed by three interrelated cameras: the principal, medial and inferior cavii. The principal cavum is the largest part of the nasal cavity; its anterior part opens into the external environment through the internal nares. Both nares, external and internal, are related to the nasolacrimal canal [9].

Nares have olfactory and respiratory functions and are situated on the anterior part of the skull, within an area surrounded by the premaxillaries, maxillaries, nasals and vomers. The skeletal structures of the nasal capsules are mostly cartilaginous, with the septomaxillaries being the only osseous structures as well as the main structural framework. A nasal septum composed of trabecular bone separates both nasal cavities along their whole length. Each nasal capsule has openings or fenestras through the septum. Due to extensive cartilague reabsorption, *Rana temporaria* has a single fenestra [10]. Narin closure in frogs is not achieved by narin-specific muscles, but through the action of the submentalis muscle in the lower jaw, whose movement is transmitted to the snout via bone and cartilage thanks to a complex relationship between the mentomenckelian, the premaxillaries and the

alary cartilages. When the submentalis muscle is relaxed, the intrinsic elasticity of the alary cartilages restores the aperture of the nares. The result is a lever system actuated by striated muscles that interrupts airflow [11].

C. Vocal sacs: the term "vocal sac" is applied to the association of three separate structures: **i:** The internal lining of the sac, a mucous membrane originated as an evagination of the mouth floor. It is communicated with the mouth cavity through one or more small openings situated laterally to the tongue. **ii:** Layers of muscle in the ventral (intermandibular muscle), posterior (interhyoid muscle) and dorsal (geniohyoid and sternohyoid muscles) faces. The association between these muscles allows the expanding and contracting the sacs. **iii:** The gular skin, which is pleated or forming lateral bags in the case of frogs with external sacs, or unmodified when internal sacs are present [12]. Our studied populations of *Rana temporaria* have internal vocal sacs, which are displayed by some males when emitting underwater calls.

D. Tympanic cavities: the tympanic cavities are air-filled diverticula of the pharynx. They have a conical shape, its base being the tympanic membrane and their vertex a short broad tube that connects to the cavity (Eustachian tube) [13]. A significant fraction of the sound that arrives to the tympanic membrane is transmitted from the oral cavity as a result of a combination of the body wall transfer function, the glottis and the tympanic structures. The multimodal energy distribution of the note is not originated in the glottis, butis a result of post-glottal filtration. Tympanic membranes are therefore important components of call radiation in amphibians, as seen in bullfrog and also *Rana temporaria* [6,14,15].

E. Larynx and Vocal Cords: the larynx in anurans is a complex cartilaginous structure. A ring-shaped cartilage (cricotracheal cartilage) is the base for two arytenoid cartilages, to which vocal cords are attached. When the glottis is closed, the medial edges of the arytenoid cartilages are in contact, which produce silent phases. The larynx dilator pivots the arytenoids over their articulations with the cricoid to open the glottis, and producing acoustic clicks.

The rapid oscillations caused by this mechanism are responsible for call structure [16] producing the characteristic "vibrator note" (croak) present in *R. temporaria*.

When emitting a release call, the movements of the chest and the larynx are of lower amplitude and duration than the equivalent during pulmonary respiration. They are also produced in two distinct phases: an initial one with incomplete and cyclical opening and closing of the glottis (vocal phase) when the call is produced, and a second with a single opening and closing (respiratory phase) [17]. The calling sounds of frogs depend on the active movement of the anatomical parts of the larynx within its skeletal framework, on the airflow generated by the lungs, and on the viscoelastic properties of the oscillating vocal cords. The laryngeal muscles move the vocal cords to a basic position, while the airflow generated by pulmonary pressure makes them vibrate. The differences in size, shape and composition of the vocal cords highly influence call frequency [18]. The speed of the wave produced is proportional to the oscillation speed of the vocal cords, which in turn depends on their elasticity. The cord model predicts that the fundamental frequency of the vocal cord is directly proportional to the square root of the relation between stress (force per unit of surface) and tissue density (estimated at 1.02 g/cm^3), and inversely proportional to double the length of the cord [19].

The purpose of our current study was to build a computational model of the *R. temporaria* release call that takes into account the role of those anatomical elements that influence call structure, such as the mouth and nose cavities, the vocal sacs, the tympanic cavities and the larynx with the associated vocal cords. We set as the basis of our computational model two assumptions:

- The mouth cavity of frogs can act as a Helmholtz resonator, both above and under water, which is tuned to a specific frequency and suppresses specific frequency groups, in a similar way to those used in architectural acoustics. Such a role on shaping the characteristics of a call would make mouth shape and size selective characters.
- The nose cavity acts as a tube resonator, reinforcing higher frequencies when the calls are emitted above water.

Material and Methods

All the data was collected in the field at the Pyrenees mountains. Great care was taken to minimize stress for the tested frogs.

Photographs

During the end of July and the beginning of August 2014 we took data from 373 individuals of *R. temporaria*. All individuals were older than one year, 37 of them were breeding adults. Neither the morphological (no visible secondary sexual characters) nor the genetic [sex reversal dependent on temperature sex of the other sub-adult

frogs could be determined [20]. We sampled 30 locations in the southern slope of the central Pyrenees (Figure 2 blue). Frogs were kept constantly wet for 30-60 min in a fine cloth bag before being photographed on top of a white portable grid (for scale adjustment) with a Canon Power shot SX260 HS digital camera. All pictures were taken between 12:00 and 14:00 in full sunlight on days with no overcast cloud cover and the camera was set to auto-expose all images in order to minimize any effects of differing ambient illumination and to generate consistently exposed photographs. For each frog, photographs from dorsal, ventral and lateral views were taken. After photographs were taken, juvenile frogs were immediately released without further manipulation, while adults were used in the induced vocalization protocol.

Calls

For each of the recorded vocalizations, we used Sound Forge Pro 10.0 (Magix Software GmbH, Berlin, Germany) to separate individualized croaks that were saved in*. Wav format (Figure 1) and normalized by considering the largest peak as 100% amplitude in order to compare them.

Matlab code 1:

$$y = y / \max(y)$$

Above-water call recording: The samples used for the development of our analysis methodology were taken from individuals of *Rana temporaria* from the Central Pyrenees in the summer of 2013 (Figure 2 red) and 2014 (Figure 2 blue). We aimed to record release calls, which are produced by both male and unreceptive female frogs when grasped by male frogs [21]. This type of vocalization can be easily induced by gently grabbing the frog and results in little to no damage or stress for the animal [22]. Vocalizations were recorded using a TCD-D8 Portable Digital Audio Tape (Sony Corporation, Tokyo, Japan) a directional microphone (C568B, AKG acoustics, Vienna, Austria) with integrated amplifier and 20-20.000 Hz bandwidth. Sampling rate was 44.1 kHz.

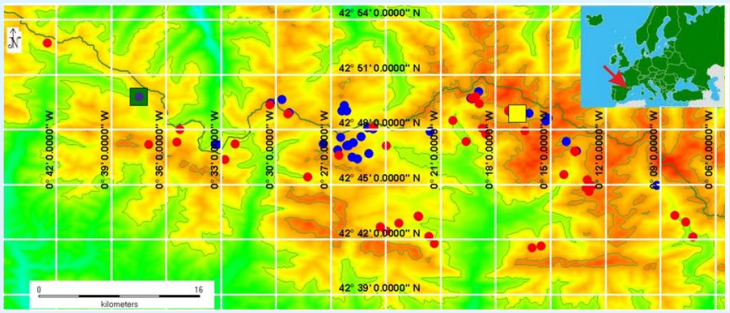

Figure 2: Sampled locations in the central Pyrenees. Blue points: frogs photographed on top of a white portable grid (for scale adjustment) and recordings of induced release calls of adult frogs (2014). Red points: recordings of induced release calls in adult frogs (2013). Yellow Square: Ibon de las Ranas in the Respomuso valley, recordings of induced calls in adult frog's under-water (2016) and radiographs of frogs in the Respomuso lodge (2001). Green square: Aguas Tuertas, recordings of under- and above–water induced release calls of an individual (2016) and an unusual and spontaneous above-water release call during the post-breeding season (2014).

Underwater: During the second half of July and the first half of August 2016, we sampled 149 underwater induced notes from 19 frogs at the Ibon de las Ranas in the Respomuso valley (Figure 2 yellow square). The protocol was similar to the one used for above-water notes, but we used a sub-aquatic video camera (Sony JVC, GZ-RX15) to record both image and sound.

Exceptional Vocalizations

The following are vocalizations that were not part of our systematic recordings, but they were preserved and analyzed for their interest.

During the first fortnight of August 2014, at Aguas Tuertas (Figure 2 green square), a male vocalized spontaneously (which is unusual in our sampled area during the post-breeding season) while in a cloth bag with other males that were waiting for their turn in the induced vocalization tests. A single croak from the aforementioned male was recorded while the directional microphone was pointing at the bag. During the first fortnight of August 2016, also at Aguas Tuertas, we recorded underwater (23 notes) and above-water (48 notes) vocalizations from a male.

X-Rays

During July and August, 2001, 26 frogs were radiographed at the Respomuso Lodge (Figure 2 yellow square) where we installed an X-Ray System (2100 Intraoral X-Ray System, Kodak, New York, USA) in order to take radiographies without transporting frogs for long distances. Frogs were massaged lightly with a finger on the throat area, which relaxed them for the few seconds necessary to take the picture.

Note Simulation

Taking a spontaneous vocalization (release call) from a male as a baseline, we extracted the duration in ms (leng), sampling rate (fs) and fundamental frequency (F0). Using these parameters, we can calculate a vector representing a simple note (Figure 3(B1)).

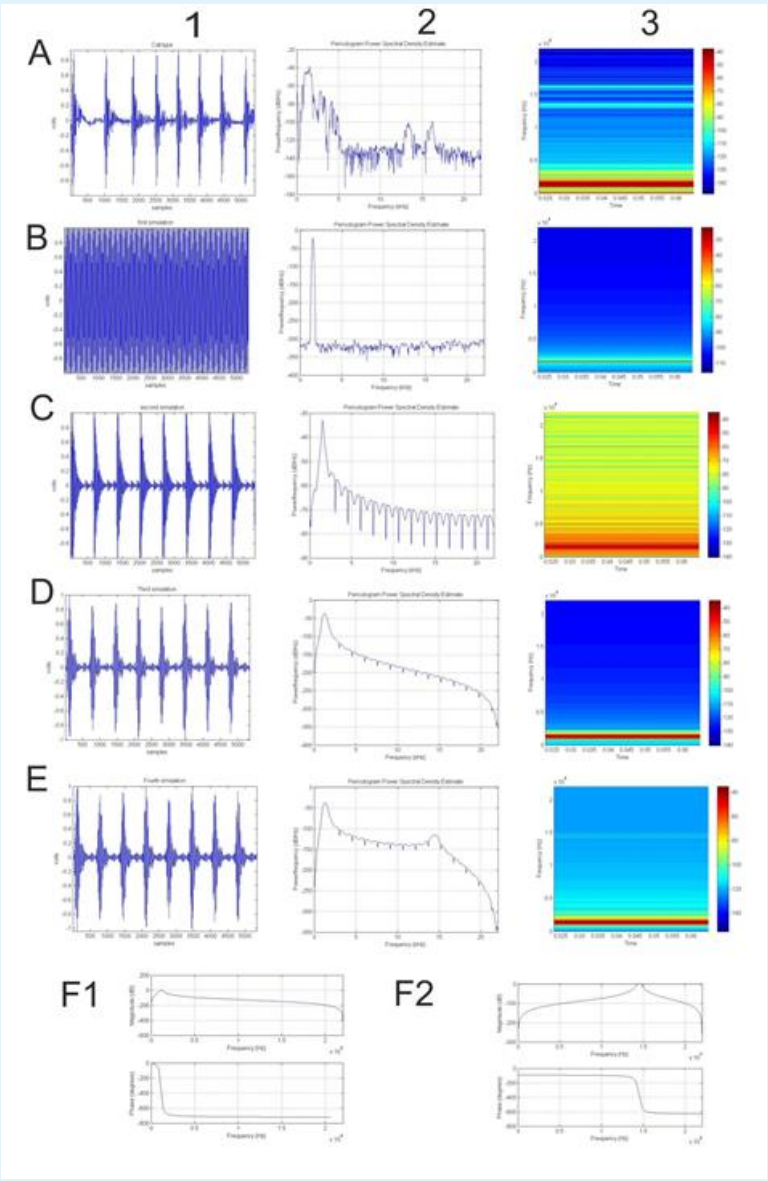

Figure 3: A: Oscillogram, period gram and spectrogram of the spontaneous call of a male; **B:** simulated pure note; **C:** tremolo obtained from B via an amplitude filter; **D:** simulation obtained via the application of the first Butterworth filter to C; **E:** final simulation obtained by applying the second Butterworth filter to D; **F1:** amplitude and phase response of the first Butterworth band pass filter; **F2:** amplitude and phase response of the second Butterworth band pass filter.

Matlab code 2:

$$Ts = 1/fs$$

t=0:Ts:leng; y=sin(2*pi*F0*t); plot (y,'MarkerSize',5); axis tight; xlabel('samples'); ylabel('volts');

We can modulate the amplitude of this simple note, making the sound fluctuate n times, where n is the number of peaks per note (recorded as a variable named modules in our code) while keeping F0 constant. In this way, we obtain a tremolo effect. Such a fluctuation with a fixed F0 and a harmonic series defines the typical timbre of frog vocalizations, which we will name "croak" from now on in order to distinguish it from a pure note. Croak creation is handled by a custom amplitude filter:

Matlab code 3:

[y,fs]= audioread(filename); PP=pulseperiod(y,fs); p=size(PP,2); S=size(y); ns=S(2); mp=round(ns/p); est=round (ns/nmodules);estep=est; pasa=1;grava=1;md=1;mpp=1; c=1; c1=1; Vy=y';for a=1:ns; if a==estep pasa=pasa+1; estep=est*pasa; md=1;% c=c+1; c1=1; c=1; else; end; mpp=mpp+1; if c1>2 c=0.7; else; end; if mpp> mp md=(md*c); mpp=1;c1=c1+1; else; end; if md < 0.01 md=0.08; else; end; Vy(a)=Vy(a)*md; end; Vr=Vy'; plot (Vr,'MarkerSize',5);axis tight;xlabel('samples'); ylabel('volts'); title('second simulation');

Once the croak is created, we apply LTI (Linear Time-Invariant) filters in order to:

- Modify the frequency spectrum of the croak, fitting it to the baseline as closely as possible. For this, we use two serial Butterworth Infinite Impulse Response filters with different parameters, which yield different magnitude and phase outputs. For the first filter (Figure 3, F1) the band-pass parameters for the buttord Matlab function are: fstop1=1; fpass1=1000; fpass2=1300; fstop2=1500; Rp=3; Rs=22. For the second filter (Figure 3, F2) the parameters are: fstop1=13000; fpass1=14000; fpass2=15000; fstop2=15500; Rp=18; Rs=26.
- Obtain representative plots (periodograms and spectrograms) that facilitate the comparison of our simulations to the baseline vocalization. To this end, we used Kaiser Finite Impulse Response windowed filters (code 4) as well as Burg filters with 20 sensitivity (code 5).

Matlab code 4:

[y,fs]= audioread (file); spectrogram(y, kaiser (2048,5),220,512,fs,'yaxis'))

Matlab code 5:

pburg (yt,20,2500,fst);

Comparison between Sound and Anatomy

In our first approach to explore the relationship between anatomy and sound, we used pictures from 35 adult frogs (25 males with SVL= 6.14±0.64 cm and 10 females with SVL= 5.675±1.26 cm) as well as the radiographs taken from 26 frogs of different sizes taken in situ close to their reproduction sites in high mountain (Figure 4).

The photographs showing the head profiles of each frog were studied using custom template designed using GeoGebra software (Figure 5(A)). The bases of this template are 3 concentric circumferences: the smallest one fits to the eye perimeter, the intermediate is fit to the external nares, and the largest is fit to the snout. The center of the tympanic membrane is approximated to a point of the intermediate circumference; from this point, another circumference is fit to the perimeter of the tympanic membrane. A vector (AI) is fit to one of the sides of a square from the grid (known to be 0.5 cm long) in order to calculate the scale and be able to calculate absolute sizes from the relative distances of the templates. The variables calculated were: T1T2= diameter of the tympanic membrane, O1O2= eye diameter, O2N= distance between the edge of the eye and the narin, NM= distance from narin to snout. Variables were saved in an SPSS data sheet to be processed.

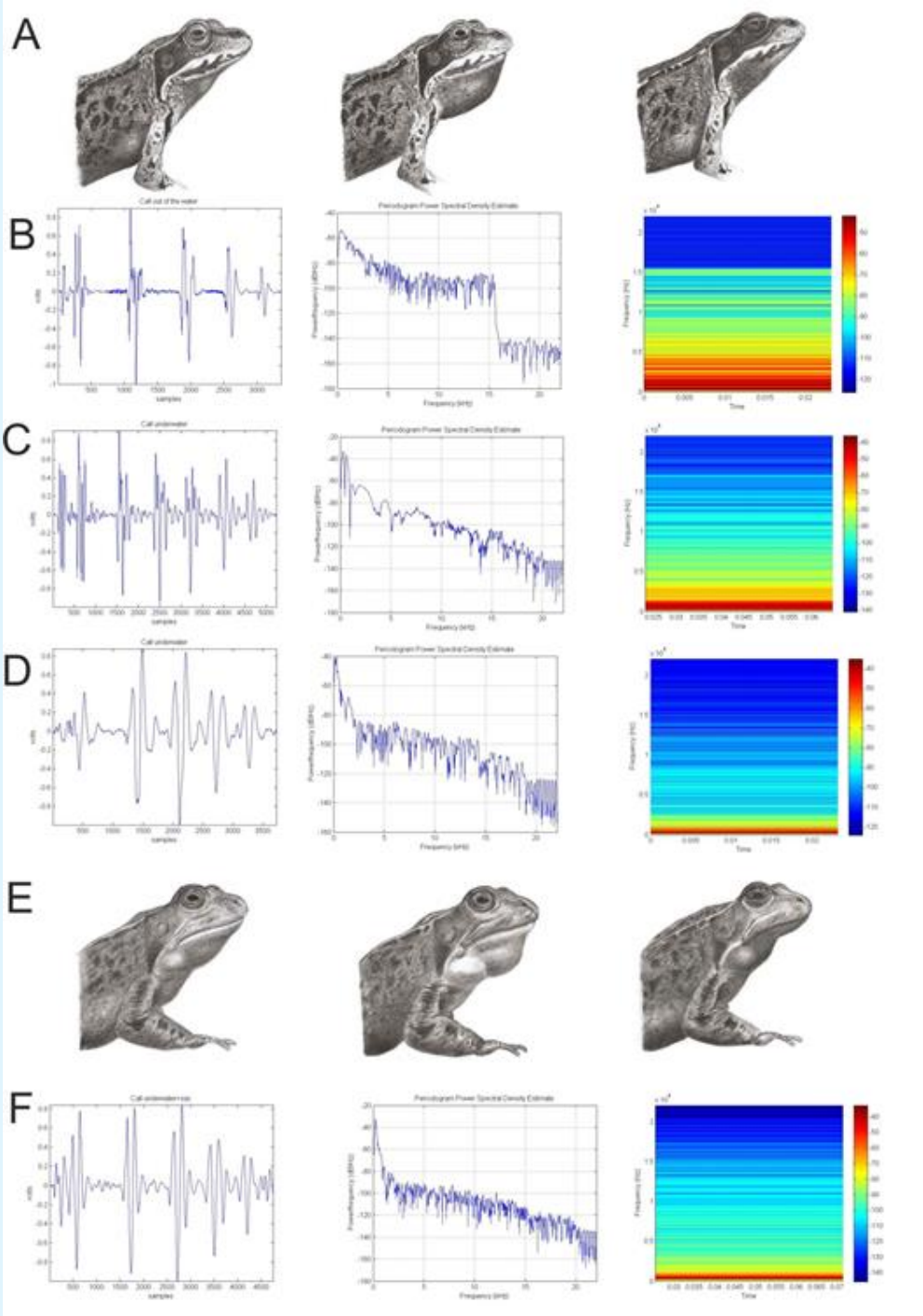

Figure 4: A: representation of a frog calling without using the internal vocal sacs; **B:** above-water vocalization of the male individual identified as AT; **C:** underwater vocalization of AT; **D:** underwater call with no vocal sac display by the male identified as RE1; **E:** representation of a male frog displaying vocal sacs; **F:** underwater call with vocal sac display by RE1.

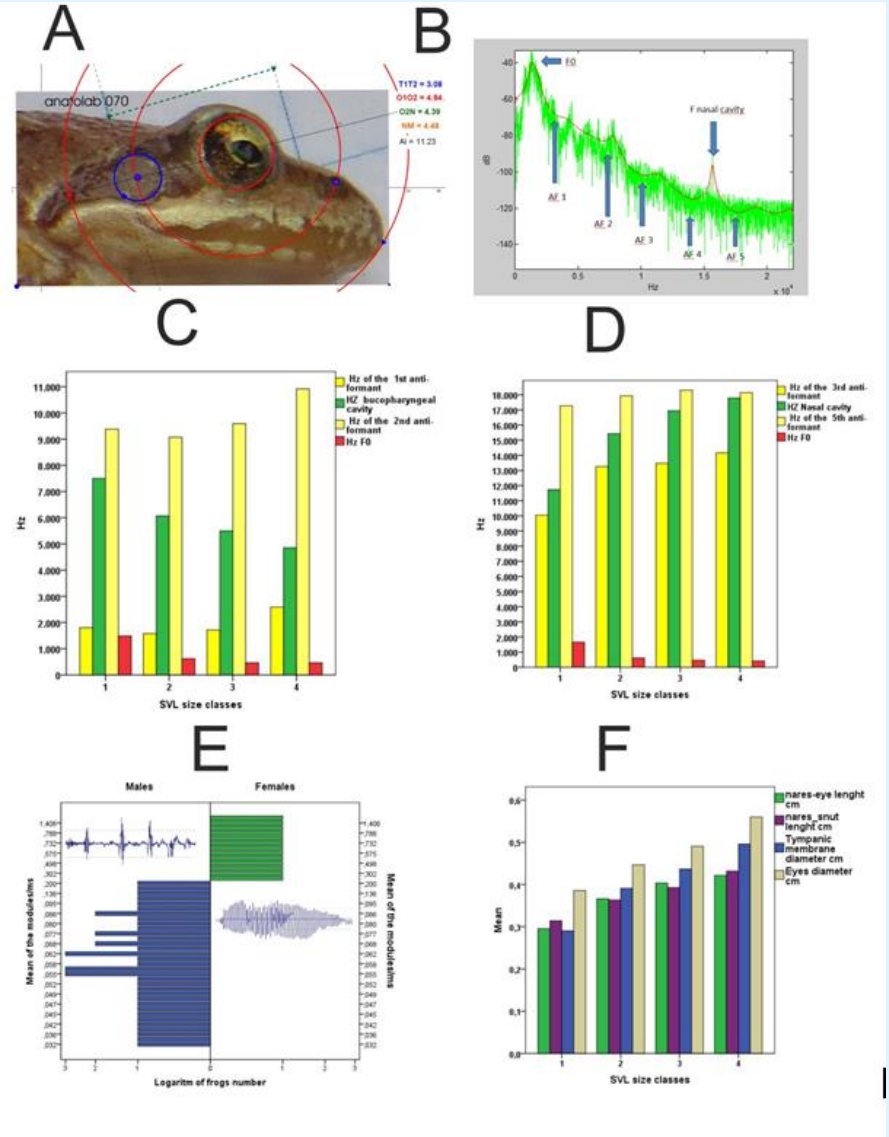

Figure 5: A: Template designed with the GEOGEBRA software. This template is composed of three concentric circumferences (red) and an eccentric circumference (blue). The blue circumference marks the perimeter of the tympanic membrane (T1T2 diameter). The smallest red circumference fits the perimeter of the eye (O1O2 diameter). The medium circumference passes through the external nares, and the largest is adjusted to the snout. Together, these circumferences define the eyes-to-narin (O2N) and snout-to-narin (NM) distances. The AI distance is equivalent to the 0.5 cm reference reticule distance, and is used to calculate the absolute values for the other distances. **B:** periodogram that shows the frequencies of the formants and anti formants for a typical above-water induced call. A Burgh-type window is indicated in red, and the Fourier transform is depicted in green. **C:** representation, for 4 frog size classes, of the Hz corresponding to the first and second anti-formants (yellow bars), the Hz of the Helmholtz resonator calculated from the volume of the mouth cavity (green bars) and the fundamental frequencies of the vocalizations (red bars). **D:** representation, for 4 frog size classes, of the Hz corresponding to the third and fourth anti-formants (yellow bars), the Hz of the tube resonator calculated from the length of the nose cavity (green bars) and the fundamental frequencies of the vocalizations (red bars). **E:** plot showing the differences in peaks-per-second between sexes and individuals. The x axis shows the number of frogs on a logarithmic scale, the Y axis shows the value of the peaks-per-second variable; **F:** comparison of the studied morphological variables between the different frog size classes.

For each analyzed frog, we added to the databank the following variables, which express numerically some of the characteristics of the call period gram:

➢ The first harmonic named fundamental frequency (F0) (Code 6).

Matlab code 6:

[r,harmpow,harmfreq] = thd(yt,fst,14); F0=harmfreq(1,1);

➢ Value in Hz of the first 5 anti-formants. Calculating the difference between the periodogram fits obtained with values of the Burg algorithm 2 sensitivity from the one with 20 sensitivity. As a result we obtained a differential curve. Peaks in the differential curve with a value over the fit larger than a threshold (5 in our case) were considered anti-formants (Code 7).

Matlab code 7:

[x,Fs]= audioread (filename); [xRB2, FB] = pburg (x, 2, 2500, Fs); curva2 = 10*log10(xB2); [xB20, FB]= pburg (x, 20, 2500, Fs); curva20 = 10*log10(xB20); antiformantes = curva2-curva20; [pksx, locsxaf]= findpeaks (antiformantes, 'MINPEAKHEIGHT', 5); Herzios= FB(locsxaf); Hz5= Herzios(1:5,1);

➢ Peaks per note (Code 8).

Matlab code 8:

[x,Fs]= audioread (filename); DB=db (xR); POT= db2pow (DB); [pk,loc]= findpeaks (POT, 'MINPEAKHEIGHT',0.1); [pM,loM]= findpeaks (pk, 'MINPEAKHEIGHT',0.3); nmodules= size(loM,1);

In addition, we added seven other variables corresponding to the location, year, month and day of sampling as well as the species, snout-vent length and physical sex of the individual.

We created a database of complementary period grams of all the notes from the same frog to examine the differences in vocalization structure between specimens. From these, we constructed a series of periodograms for each specimen that included as the independent variable the values of the frequency in Hz, and as dependent variable the Burg algorithm with 50 sensitivity. Power/frequency values (dB/Hz) were used to calculate the mean, minimum, maximum and typical deviation of the intensity.

Under our first assumption that the mouth cavity can act as a Helmholtz resonator by absorbing specific frequencies, we calculated its properties by using the formula: f = (s/2* pi) (sqrt{a/(l *v)}) [23]. In this formula f=resonance frequency; s=speed of sound through air; a=neck area; l=neck length; v= volume. Considering the mouth cavity as a rectangular prism (Figure 1) and using the measures from our pictures, we calculated each side (LH=2*O_2N+O1O2+NM cm) and its height (AV= sqrt(LH^2/2) cm). As width can be assimilated to side length, the volume of the mouth cavity can be defined as v= (O_2N*AV^2)/2) cm^3. Neck radius, assuming a circular cross-section, was estimated as $O_2N/2$, and therefore area was defined as a= pi*($O_2N/2$)^2 cm^2. Length was calculated as l= T1T2 cm. Under high-mountain conditions (dry air, 10ºC) sound velocity through air is c= 33750 cm/sec.

Under the second assumption that the nasal cavity acts as a tube resonator open on two ends that reinforces specific frequencies, we performed the calculations based on the formula F=nc/2L. In this formula, F is the reinforced frequency in Hz; n is an integer (we set it to 1, the lowest possible value); c is sound velocity through air which, as before, is set to 33750 cm/sec; L is the length of the nasal cavity in cm, which we estimated using our radiographs as (O_2N*2)+(NM/2), O_2N being the length in cm from the narin to the edge of the eye, and NM the length in cm from the narin to the tip of the snout.

Considering the vocalizations of all our studied individuals, we compared them to their anatomy by contrasting the frequencies observed in the formants and anti-formants in our recordings (Figure 5(B)) with the theoretical frequencies calculated with the measured anatomical dimensions. For this purpose, we divided our individuals into four size classes according to their SVL: size 1 (4-4.9 cm), size 2 (5-5.9 cm), size 3 (6-6.9 cm) and size 4 (7-7.9 cm).

Results

We obtained an oscillogram, periodogram and spectrogram of a spontaneous call from a male (Figure 3(A)), which we used as a template, as well as the values corresponding to call duration (121 ms), sampling rate (44100 Hz) and the fundamental frequency (1534 Hz). The oscillogram and periodogram showed 8 peaks per note, and the spectrogram showed two formants between the 1000 and 3000 Hz, and another two between the 12000 and 17000 Hz. A large anti-formant was placed between the two formant groups. Using the values corresponding to the duration, sampling rate and fundamental frequency, we created a pure tone (Figure 3(B)). The periodogram and the spectrogram showed a single formant at the established fundamental frequency (1534 Hz). From this pure tone, and using our amplitude

filter, we obtained a tremulo with the same number of peaks per note as the template (nmodules = 8) and the same fundamental frequency. We found a large number of harmonics of power between -60 and -80 dB (Figure 3(C)), whilst in our template they were located between -80 and -140 dB. The timbre of this tremulo is very similar in sound to a croak, but both the periodogram and the spectrogram show a smooth, constant decline in the dB values of the harmonics, without distinct formants or anti-formants.

The first step in our simulation process was to keep the fundamental frequency below -40 and -50 dB, while lowering the harmonics below -120 dB. To this end, we applied a first band-pass Butterworth filter to our synthetic tremulo (Figure 3(F1)). The magnitude and phase profile of our filter reduced the power of any harmonics beyond the first two (Figure 3(D)) while altering as little as possible the fundamental frequencies, which changed from 1534 to 1273 (a 261 Hz change). The oscillogram remained constant for under- and above-water notes.

By applying a second band-pass Butterworth filter (Figure 3(F2)), we obtained a simulation (Figure 3(E)) that closely resembled the template in its basic amplitude distribution and its fundamental frequency (1339 Hz versus the 1534 Hz of the template). Formants and sntiformants were also similar, with an anti-formant located between the 5000 and 10000 Hz and two formants located at the fundamental frequency and15000 Hz, respectively. This iteration of the simulation presented a very similar timbre to our template.

The individuals of *Rana temporaria* in our study area did not vocalize spontaneously above water. The only spontaneous call we recorded, the one we used as template for our simulation, was produced by a frog tightly grouped with others inside a cloth bag, which was half-submerged in a stream while we prepared the photographic and video recording equipment. During our monitoring of this population (from 1996 to 2017), we have only been able to record induced release calls above water. Considering this, we took video recordings of release calls that were induced while under water, from which we selected two belonging to two male frogs (AT and RE). The AT male emitted induced vocalizations both below- and above-water. On the other hand, males in our study area only displayed their internal vocal sacs when calling under water, and even then only on some occasions; the RE male was recorded for several minutes vocalizing underwater with (Figure 4(A)) and without (Figure 4(E)) vocal sac display. We observed and compared these two vocalizations carefully.

When comparing the calls the AT individual performed above (Figure 4(B)) and below water (Figure 4(C)), we could observe the following differences: **1:** Fundamental frequency above water was 3348 Hz, while below water it was 3090 Hz. **2:** There was a small anti-formant between the 5000 and 14000 Hz for the above-water call that was absent in below-water calls. **3:** There was a formant close to 15000 Hz above water that was absent below water.

When comparing the calls from the male that called below water both with and without vocal sacs (Figure 4(D) with sacs, Figure 4(E) without), we found small differences between the power of the harmonics and the fundamental frequency, which was reduced from 2486 to 2228 Hz when vocal sacs were exhibited.

In Figure 5(B) we present a periodogram where the frequencies for both formants and anti-formants in a typical vocalization are shown. Red shows a Burg window, and green shows the Fourier Transform. The periodograms of all frogs studied during 2013 and 2014 (corresponding to induced, above-water vocalizations) show that the position of formants and anti-formants is consistent between individuals, while their power fluctuates depending on the specific individual. As shown in our model, the role of the mouth cavity in calling frogs can be assimilated to a Helmholtz resonator that absorbs and dampens specific groups of frequencies. Figure 5(C) shows that the dampened frequency group, as calculated according to our model (green bars) always fall between the frequencies of the two first anti-formants (first and second yellow bars). The frequency group affected by the mouth anti-formant decreases as frog size increases, which is also the case with the fundamental frequency (red bars). All of these characteristics closely resemble those of the recorded calls. On the other hand, our data also show that the nose cavity acts as a tube resonator that increases the power of certain frequencies. Figure 5(D) shows that this reinforced frequency group (green bars) always falls between the third and fourth anti-formants (yellow bars), and that its median frequency increases with frog size.

Discussion

Our simulation of *R. temporaria* calls starts with a pure note (Figure 3(B)), which in the living frogs originates in the vibration of the vocal chords due to the airflow

generated by pulmonary pressure [18]. The cord model predicts that the fundamental frequency (F0) of a vocal cord is inversely proportional to double the length of the chord, and directly proportional to the square root of the ratio between stress and tissue density, the latter being a constant when studying a single species [19]. In practice, this means that larger frogs should have a lower F0 (Figure 5(C), red bars), which will result in an easier propagation through the medium, since higher frequencies suffer more attenuation from small objects in the environment. Adult frogs within our study population had an SVL between 4 and 8 cm in length, and a F0 between 18 and 5909 Hz (from 2152 croaks belonging to 55 frogs) which is very far from the call frequencies that have been reported previously for *R. temporaria* [24], where the fundamental frequency band extends from 300 to 900 Hz, with a distinct maximum between 350 and 500 Hz. However, and despite there being a clear trend for frogs of larger sizes to emit calls of lower F0, we did not found a clear correlation between a croak's F0 and the size of the caller, since both males and females in our population can emit croaks with very different F0. This indicates that other factors, most likely control of vocal cord length during phonation [19] influence the final F0 of a given call. Once the pure note is generated in the vocal cord, it must be transformed into a tremulo (the characteristic "croak") with a certain number of peaks per note depending on the individual (Figure 3(C)). In our data (acoustic database from the study of 2152 notes from 55 frogs) the number of peaks per note averaged 5.6 ± 4.1 for males and 53 ± 39.9 for females, which makes it the variable that better separates males and females (Figure 5(E)). The rapid oscillations produced by the opening and closing of the glottis during the vocal phase when the croak is generated are the main determinant of the number of peaks per note [16,17].

The next step in building the simulation was to drastically reduce the power of frequencies from the third harmonic onwards (Figure 3(A)), as well as slightly lowering F0 and increasing its power (Figure 3(D)). We achieved this by the use of a Butterworth filter, as described in methods (Figure 3(F1)). This reduction in the power of the harmonics, which in our data oscillates between a minimum of 734 Hz for the first anti-formant and a maximum of 15400 Hz for the second anti-formant depending on the individual, is the consequence of the anatomy of the mouth cavity acting as a Helmoltz resonator (Figure 5(C)) and absorbing a group of frequencies that depends on the volume of the specific mouth cavity. Mouth cavity volume is increased during vocalization, especially when male individuals expand their internal vocal sacs Figures 4(A) & 4(D) with no vocal sacs, 4(E) & 4(F) with expanded vocal sacs. The decrease in power of certain frequencies by the anti-formants caused by the mouth cavity reduces noise and highlights the F0, which makes mouth cavity size a potential target for sexual selection.

In our studied vocalizations we also observed a substantial increase of the power of some frequencies, with a clear formant appearing between the third and fifth anti-formants at 11000 and 20000 Hz respectively (Figure 5(B) & 5(D)). In our simulation (Figure 3(E)) we achieved these effects using a second Butterworth filter (Figure 3(F2)). We were not able to explain this formant, consistently present in the spectrograms and periodograms of the inducted vocalizations until we were able to record induced vocalizations below water and compared them to above-water calls from the same individual (Figures 4(C) & 4(B)). In the case of below-water calls, the aforementioned formant disappeared, while the only noticeable behavioral difference was that frogs closed their nares while vocalizing. Therefore, our assumption that the nasal cavity (Figure 1(B)) acts as a tube resonator reinforcing certain sets of frequencies depending on the length of the tube (represented by the inner nasal cavity) is confirmed. However, the adaptive value of nose cavity size is hard to evaluate, as higher frequencies transmit poorly through the environment. Moreover, although their particular formant is characteristic of above-water vocalizations, our study populations do not usually vocalize above water. We can therefore conclude that the structural properties of the call of *Rana temporaria* depend on: **1:** the size of the frog, which influences the fundamental frequency. **2:** the ability to produce rapid oscillations via opening and closing the glottis, modulating the amplitude of the call and giving it its characteristic croak timbre (note vibrator). **3:** the reinforcement of the fundamental frequency thanks to the role of the mouth cavity as a Helmoltz resonator.

Conclusion

In summary, the computational model developed in this paper was able to replicate the main characteristics of *R. temporaria* release call common to all individuals of the species. We were also able to identify the portions of the call that present the largest individual variation (namely, the dB power and fine position of formants and anti-formants).

We successfully created a model that reproduced the general structure of the release call of *R. temporaria*. The

model integrated the influence of the mouth and nose cavities, and will be used as a base for a more complete bioacoustics characterization and monitoring of our study populations.

We were also able to find clear differences between male and female release calls, as well as determining which characteristics of the call are species-specific and which of them show individual variation. We present this model as a useful bioacoustics tool that can be used to monitor our study population alongside more traditional methods.

Acknowledgment

This project was supported by the Animal Anatomy Laboratory Foundation (2013-302). We thank Ursicino Abajo, warden of the Respomuso mountain refuge, for his logistic and gastronomic support, and the field assistant volunteers during the summer courses.

References

1. Avila RW, Pansonato A, Perez R, Carvalho VTD, Roberto IJ, et al. (2018) On Rhinella gildae Vaz-Silva, Maciel, Bastos & Pombal 2015 (Anura: Bufonidae): Phylogenetic relationship, morphological variation, advertisement and release calls and geographic distribution. Zootaxa 4462: 274-290.

2. Marquez R, Beltran JF, Vaca IP, Samlali MA, SKhifa A, et al. (2018) Release calls of Moroccan spadefoot toad, *Pelobates varaldii* (Anura, Pelobatidae). Amphibia Reptilia 39(3).

3. Stanescu F, Forti LR, Cogalniceanu D, Marquez R (2019) Release and distress calls in European spadefoot toads, genus Pelobates. Bioacoustics 28(3): 224-238.

4. Christensen Dalsgaard J, Breithaupt T, Elepfandt A (1990) Under water hearing in the clawed frog, Xenopus laevis. Tympanic motion studied with laser vibrometry. Naturwissenschaften 77(3): 135-137.

5. Narins PM, Feng AS, Fay RR, Popper AN (2007) Hearing and Sound Communication in Amphibians.

6. Hoyos JM, Sanchez Villagra MR, Carlini AA, Mitgutsch C (2012) Skeletal development and adult osteology of Hypsiboas pulchellus (Anura: Hylidae). Acta Herpetol 7(1): 119-138.

7. Laloy F, Rage JC, Evans SE, Boistel R, Lenoir, et al. (2013) A re-interpretation of the Eocene anuran *Thaumastosaurus* based on microCT examination of a 'mummified' specimen. Plos One 8(12).

8. Nowack C, Wohrmann Repenning A (2010) The nasolacrimal duct of anuran amphibians: suggestions on its functional role in vomeronasal perception. J Anat 216(4): 510-517.

9. Pugener LA, Maglia AM (2007) Skeletal morphology and development of the olfactory region of Spea (Anura: *Scaphiopodidae*). J Anat 211(6): 754-768.

10. Gan C, Pyles R (1983) Narial closure in toads; which muscles?. Respir Physiol 53: 215-223.

11. Elias Costa AJ, Montesino R, Grant T, Faivovich J (2017) The vocal sac of Hylodidae (Amphibia, Anura): Phylogenetic and functional implications of a unique morphology. J Morphol 278: 1506-1516.

12. Mason MJ (2007) Pathways for sound transmission to the inner ear in Amphibians. In: Hearing and Sound Communication in Amphibians, edited by Narins PM, Feng AS, Fay RR, Popper AN (Springer Handbook of Auditory Research, vol 28. Springer, New York, 2007) Chapter 10: 147-183.

13. Vlaming MSMG, Aertsen AMHJ, Epping WJM (1984) Directional hearing in grass frog (*Rana temporaria* L): I Mechanical vibrations of tympanic membrane. Hear Res 14(2): 191-201.

14. Purgue AP (1997) Tympanic sound radiation in the bullfrog Rana catesbeiana. J Comp Physiol 181(5): 438-445.

15. Walkowiak W (2007) Call production and neural basis of vocalization. In: Hearing and Sound Communication in Amphibians edited by Narins PM, Feng AS, Fay RR. Popper AN (Springer Handbook of Auditory Research, vol 28. Springer, New York, 2007), Chapter 4: 87-112.

16. Schmidt RS (1965) Larynx control and call production in frogs Copeia 2: 143-147.

17. Brown C, Riede T (2017) An Introduction to Laryngeal Biomechanics. In Comparative Bioacoustics: An Overview.

18. Riede T (2013) Body size, vocal fold length, and fundamental frequency-implications for mammal

vocal communication Nova Acta Leopoldina NF 111, Nr 380: 295-314.

19. Wallace H, Badawy GMI, Wallace BMN (1999) Amphibian sex determination and sex reversal. Cell Mol Life Sci 55: 901-909.

20. Wells KD, Schwartz JJ (2007) The behavioral ecology of anuran communication. In: Hearing and Sound Communication in Amphibians edited by Narins PM, Feng AS, Fay RR, Popper AN (Springer Handbook of Auditory Research, Springer, New York, 2007), 10: 44-86.

21. Schmidt RS (1972) Release calling and inflating movements in anurans. Copeia 2: 240-245.

22. Matar M, Welti R (2009) Capturing the physics of Helmholtz resonators with the acoustic wave equation. Lat Am J Phys Educ 3: 127-134.

23. Brzoska J, Walkowiak W, Schneider H (1977) Acoustic Communication in the Grass Frog (Rana t. temporaria L.): Calls, Auditory Thresholds and Behavioral Responses. J comp Physiol 118(2): 173-186.

24. Jorgensen CB (2000) Amphibian respiration and olfaction and their relationships: from Robert Townson (1794) to the present. Biol Rev Camb Philos Soc 75: 297-345.